Influence of Thermal Distortion on Gravity Gradient Stabilization

Robert L. Goldman*
Martin Marietta Corporation, Baltimore, Md.

This paper is concerned with the problem of determining the influence of solar heating on the low-frequency, dynamic stability of a gravity gradient satellite. The scope of the effort includes the development of a computer program that uses a quasi-static approach for describing a satellite's unsteady orbital motion. The essential feature of the quasi-static approach is that the satellite's long, slender booms reach their thermal equilibrium position solely as a result of thermal bending without consideration of the dynamic effects of boom vibration. A nonlinear analytical model and a corresponding computer program have been developed to study the effect of absorptivity, sun angle, and hinge stiffness on the stability of a satellite's motion. Tied to this study is a requirement to explain the source of the observed anomalous unstable behavior of the Naval Research Laboratory's gravity gradient satellite 164 (NRL 164). Within the confines of a relatively narrow stability criteria, the quasi-static model provided a valid means of predicting the anomalous behavior of NRL 164. The occurrence of computed unstable responses closely resembling flight data tended to confirm that the source of the instability is related to thermal distortion and is particularly sensitive to sun angle.

Introduction

THE apparent simplicity offered by the concept of gravity gradient control of an earth orbiting satellite[1-3] has had a stimulating effect on the design of several spacecraft configurations. From an analytical point of view it seemed clear that three-axis passive stabilization of a spacecraft could be achieved through the clever use of tip-weighted extendable booms. If stability were possible, a desirable earth-pointing equilibrium attitude of a satellite could be attained solely by a judicious arrangement of these booms.[4-6]

Experience with several gravity gradient systems has indicated that unexpected destabilizing disturbances may be present that can induce excessive attitude errors or actual attitude inversions. Such anomalous motions were clearly seen in the flight data collected during a series of gravity gradient experiments conducted by the Naval Research Lab. and examined in Ref. 7. In the course of this examination, a relationship was observed between sun angle (angle between the sun's vector and the normal to the satellite's plane) and the character of a satellite's response; this observation subsequently led to the conclusion that thermal distortion is a critical factor in a satellite's dynamic behavior. Since a boom's thermal bending and twisting is related to the sun's angle on the boom, it was subsequently suggested that a satellite's stability would be greatly influenced by the thermal distortion properties of its booms.

It should be pointed out that the unpredictable behavior examined in Ref. 7 appeared to be a sustained low frequency rigid body oscillation dominated primarily by large yaw motions. This motion was apparently unrelated to the much high frequency flexural oscillations of a sun-lighted boom predicted by Frisch.[8]

Presented as Paper 74-922 at the AIAA Mechanics and Control of Flight Conference, Anaheim, California, August 5-9, 1974; submitted August 28, 1974; revised March 6, 1975. This work was supported by the NASA Goddard Space Flight Center under Contract NAS5-22230.

Index category: Spacecraft Attitude Dynamics and Control.

*Senior Research Scientist, Martin Marietta Laboratories. Associate Fellow AIAA.

It is clear that gravity gradient satellites have been suffering from an hitherto unpredictable low frequency instability associated with solar radiation. If a correct analytical model of this instability mechanism could be obtained, then the chances of designing gravity gradient satellites in such a way as to avoid the detrimental effects of solar radiation would be considerably enhanced.

The principal objective of the research reported here is concerned with the problem of ascertaining the influence of solar heating on the low frequency, dynamic stability of a gravity gradient satellite. The scope of the effort includes the development of a computer program that uses a quasi-static approach for describing a satellite's unsteady orbital motion. Tied to this objective is a requirement to explain the source of the observed anomalous unstable behavior of the Naval Research Laboratory's gravity gradient satellite 164 (NRL 164), shown in Fig. 1.

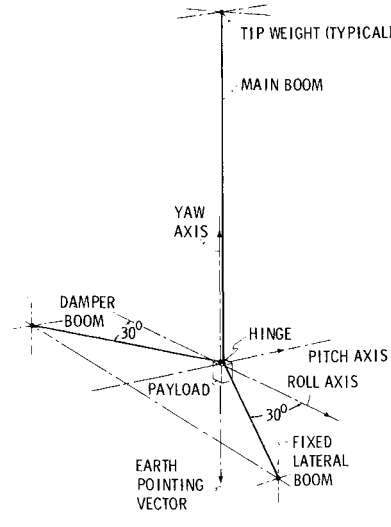

Fig. 1 Satellite geometry, NRL 164.

The quasi-static approach, based on the dynamical satellite equations described by Hooker[9] was developed as a means of simplifying the computational procedures necessary for solving the equations of motion. The approach, which is similar to that used by Kanning[10] eliminates the numerical analysis problems that arise if boom vibrations are considered. The elimination is justified by the relatively large ratio between a satellite's boom vibration frequencies and its gravity induced rigid body frequencies. In essence, boom bending is considered solely in terms of static thermal deformation. Assumptions of importance in the quasi-static approach are that: 1) The boom reaches its thermal equilibrium position solely as a result of thermal bending without any consideration of boom vibration; 2) The inertial and geometric properties of the satellite are altered as the tip weights at the ends of massless booms are displaced by boom deformation; 3) the sun line and thermal properties of a boom determine the magnitude and direction of a boom's tip deflection.

The principal disturbance mechanism considered is assumed to be due to geometrical and subsequent inertial changes resulting from thermal distortion. Thermal deformation of each of the satellite's three booms is presumed to be due solely to a thermal bending moment induced by solar heating. The resulting deformation alters the position of each boom's tip weight and, in accordance with the quasi-static approach, changes the satellite's inertial properties. As the inertial properties vary a new set of principal axes appear and reorientation of the satellite occurs. The essential question raised is: under what conditions does the resulting reorientation process become unstable?

To answer this question, the basic equations describing the rotational dynamics of NRL 164 are obtained in terms of kinematic, dynamic, orbital mechanic, and thermal distortion equations. The resulting derivation including the essential features of the quasi-static approach, leads to a set of first order, nonlinear differential equations of motion. A computer program based on this formulation has been developed and used to examine the effects of absorptivity, sun angle, and hinge stiffness on the stability of the satellite's motion.

Satellite Characteristics

The basic geometry of NRL 164 is illustrated in Fig. 1. The three-axis, two-body gravity gradient stabilization system consisted of three extendable, interlocked nonperforated booms arranged in a symmetric pattern about the plane of the pitch-yaw axes. The primary body was made up of the payload, main boom and front lateral boom (fixed to the payload); the secondary body consisted solely of the lateral damper boom. Nominally, the lateral booms were located in the horizontal pitch-roll plane. The damper boom was connected to the primary body through a single-axis hinge mechanism that constrained boom motion to a vertical plane. The hinge provided hysteresis damping torques and torsion wire spring restoring torques.

By skewing the horizontal principal axis of the damper boom out of the orbital plane, all motions become strongly coupled. Under these conditions, three-axis damping of the entire satellite is achieved by the single-degree-of-freedom motion of the damper boom about its hinge.[11]

The basic physical and thermal properties of the satellite as well as its orbital characteristics are summarized in Table 1. The booms were considered to be long, slender beryllium copper tubes with highly reflective, silver-plated outer surfaces. For the sake of simplicity the mass of the booms was ignored.

Satellite NRL 164 was stable throughout its initial period of eclipsing orbits (passage through the earth's shadow) and unstable in yaw sometime after its first excursion into a fully sunlit orbit. In fact, during the entire first passage through eclipsing orbits and first entrance into full sunlight, all attitude errors were small. The perturbations were confined to approximately one-cycle-per-orbit oscillations in pitch and ½ cycle-per-orbit oscillations in yaw.

As the satellite, in full sunlight, approached the 0° sun angle position the amplitude of the ½ cycle-per-orbit oscillations in yaw unexpectedly increased. The satellite rapidly became unstable with several yaw inversions and large amplitude oscillations in both pitch and roll. After passing through the 0° sun angle position, the instability ceased and was followed by a period of stable operation.

Simulation

For simulating the flight behavior of NRL 164 the vector dynamical equations developed by Hooker[9] are used since their application eliminates many of the difficulties common to the Lagrangian approach.[4] With respect to the basic equations, the final quasi-static attitude of the two-body satellite, including associated kinematics, dynamics, orbital mechanics, and thermal distortion, leads eventually to the problem of seeking a solution to a set of first-order, nonlinear differential equations of motion.

In the derivation of these equations that follows, boldface is used to identify a vector while a tilde is used to indicate a dyadic. Each time derivative with respect to inertial space is denoted by an additional dot over a given element.

Reference Frames

In the present case, the three orthogonal frames illustrated in Figs. 2 and 3 have been chosen. The basic inertial frame,

$$[a] = [a_1 a_2 a_3]$$

Table 1 Physical and orbital properties of NRL 164

Property	Value	Units
Lateral and damper boom tip mass	0.118	slugs
Main boom tip mass	0.159	slugs
Payload mass	8.800	slugs
Lateral and damper boom length	35.0	ft.
Main boom length	60.0	ft.
Distance from payload c.g. to hinge	1.375	ft.
Lateral and damper boom diameter	0.25	in.
Main boom diameter	0.50	in.
Lateral and damper boom wall thick	0.14×10^{-2}	in.
Main boom wall thickness	0.20×10^{-2}	in.
Payload moment of inertia	4.0	slug-ft^2
Yaw rotation of lateral boom	−30.0	deg
Yaw rotation of hinge axis	120.0	deg
Damper spring constant	0.714×10^{-3}	ft-lb/rad
Damper damping constant	0.395	ft-lb-sec/rad
Eccentricity	0.0	
Semi-major axis	7302.4	km
Earth radius	6378.2	km
Gravitational constant	3.98×10^5	km^3/sec^2
Mean orbital rate	0.1012×10^{-2}	rad/sec
Absorptivity	0.13	
Thermal coefficient of expansion	0.104×10^{-4}	in/in-°F
Thermal conductivity	4.167	Btu/hr-in-°F
Heat radiation of source	3.065	Btu/hr-in^2

is fixed in space with its origin at the earth's center. The local vertical, or orbital reference frame,

$$[E] = [E_1 E_2 E_3]$$

has its origin fixed at the satellite's center of mass and moves with it along its orbital path. The body frame

$$[e] = [e_1 e_2 e_3]$$

has its origin fixed in the satellite and is used in conjunction with the inertial frame and local vertical frame to define the satellite's motion. The nominal orientation of the undeformed NRL 164 satellite in terms of the unit vectors e_1, e_2 and e_3 is depicted in Fig. 3

The rotational position of the body frame with respect to the inertial frame is described through the orthogonal direction cosine transformation

$$\{a\} = [A]\ \{e\} \tag{1}$$

where the direction cosine elements of the matrix $[A]$ are functions of the usual Euler angles (defined here as the angles of pitch, roll, and yaw) and the true anomaly of the orbital path, ψ.

Kinematic Equations

The kinematic equations consist of the set of direction cosine rate equations that relate the elements of matrix $[A]$ to

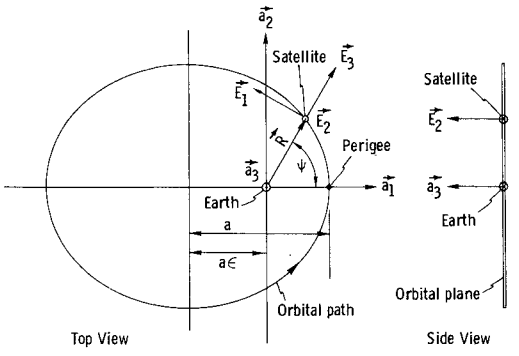

Fig. 2 Inertial and orbital reference frames.

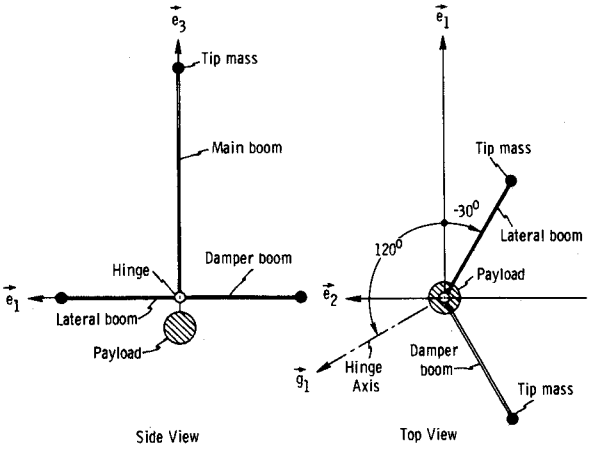

Fig. 3 Body frame and satellite orientation.

the inertial angular velocity vector, ω_0, where, in the body frame,

$$\omega_0 = \omega_1 e_1 + \omega_2 e_2 + \omega_3 e_3 \tag{2}$$

and ω_i are the body axis components of inertial rotation. For a system of moving axes the inertial derivatives of vector $\{e\}$ are given by[12]

$$\{\dot{e}\} = -[\Omega_B]\ \{e\} \tag{3}$$

where

$$[\Omega_B] = \begin{bmatrix} 0 & -\omega_3 & \omega_2 \\ \omega_3 & 0 & -\omega_1 \\ -\omega_2 & \omega_1 & 0 \end{bmatrix}$$

Since in inertial space $\{a\} = 0$, Eqs. (1) and (3) lead directly to the kinematic identity

$$[\dot{A}] = [A]\ [\Omega_B] \tag{4}$$

which when expanded yields the kinematic differential equations

$$\begin{aligned} \dot{A}_{11} &= A_{12}\omega_3 - A_{13}\omega_2 \\ \dot{A}_{12} &= A_{11}\omega_3 + A_{13}\omega_1 \\ \dot{A}_{13} &= A_{11}\omega_2 - A_{12}\omega_1 \\ \dot{A}_{21} &= A_{22}\omega_3 - A_{23}\omega_2 \\ \dot{A}_{22} &= A_{21}\omega_3 + A_{23}\omega_1 \\ \dot{A}_{23} &= A_{21}\omega_2 - A_{22}\omega_1 \end{aligned} \tag{5}$$

Only six equations are necessary since the orthogonality of the direction cosine matrix $[A]$ dictates the intrinsic values of the remaining three elements, A_{31}, A_{32}, and A_{33}.

Dynamic Equations

The complete vector dynamical equations for NRL 164 using the results of Ref. 9 can be written in the form

$$\begin{aligned} &(\tilde{\Phi}_{00} + \tilde{\Phi}_{10}) \cdot \dot{\omega}_0 + (\tilde{\Phi}_{01} + \tilde{\Phi}_{11}) \cdot (\dot{\omega}_0 + \delta g_1) = E_0^* + E_1^* \\ &g_1 \cdot [\tilde{\Phi}_{10} \cdot \dot{\omega}_0 + \tilde{\Phi}_{11} \cdot (\dot{\omega}_0 + \delta g_1)] = g_1 \cdot E_1^* \end{aligned} \tag{6}$$

As derived in Ref. 13 the dyadics $\tilde{\Phi}_{00}$, $\tilde{\Phi}_{10}$, $\tilde{\Phi}_{01}$, and $\tilde{\Phi}_{11}$ are obtained from the geometrical and inertial properties of the satellite while the torque vectors E_0^* and E_1^* arise from consideration of moments due to gyroscopic torques, gravity gradient torques, hinge-acceleration torques, gravitational forces interacting through the hinge and hinge torques due to damper rotation. In the dynamic equations, δ = the angular rotation of the damper boom about its hinge axis and, as

shown in Fig. 3, g_1 = the vector direction of the hinge axis. In matrix form Eq. (6) can be written as

$$\begin{bmatrix} \tilde{a}_{00} & a_{01} \\ a_{10} & a_{11} \end{bmatrix} \begin{bmatrix} \omega_0 \\ \dot{\delta} \end{bmatrix} = \begin{bmatrix} E_0^* + E_1^* \\ g_1 \cdot E_1^* \end{bmatrix} \tag{7}$$

Introducing the new dependent variable Δ such that $\delta = \Delta$, permits the dynamic equations [Eq. (7)] to be expanded into the scalar form

$$\begin{bmatrix} I_{11} & I_{12} & I_{13} & I_{14} & 0 \\ I_{21} & I_{22} & I_{23} & I_{24} & 0 \\ I_{31} & I_{32} & I_{33} & I_{34} & 0 \\ I_{41} & I_{42} & I_{43} & I_{44} & 0 \\ 0 & 0 & 0 & 0 & 1 \end{bmatrix} \begin{bmatrix} \dot{\omega}_1 \\ \dot{\omega}_2 \\ \dot{\omega}_3 \\ \Delta \\ \dot{\delta} \end{bmatrix} = \begin{bmatrix} T_1 \\ T_2 \\ T_3 \\ T_4 \\ \Delta \end{bmatrix} \tag{8}$$

where T_1, T_2, and T_3 are the magnitudes of the torque vectors about each of the body frame coordinates and T_4 is the torque acting about the damper boom hinge axis.

Orbital Mechanics

The orbital path of the satellite is derived directly from the solution of Kepler's equation based on a spherical earth model. This solution is carried out under the assumption that perigee occurs at $t = 0$ at which time the orbit path crosses the inertial a_1 axis. Referring to Fig. 2 the complete formulation of the decoupled Keplerian orbit is given by the first-order differential equation

$$\dot{\Psi} = \frac{\Omega_0}{(1-\epsilon^2)^{3/2}} (1+\epsilon \cos \psi)^2 \tag{9}$$

where $\Omega_0 = (\mu/a^3)^{1/2}$ = mean orbital rate, a = semi-major axis, ϵ = orbital eccentricity, μ = gravitational constant, ψ = true anomaly.

Thermal Deformation

Thermal deformation of each of the satellite's three booms is presumed to be due solely to a thermal bending moment induced by solar heating. The resulting deformation alters the position of each boom's tip weight and, in accordance with the quasi-static approach, changes the satellite's inertial properties. As the inertial properties vary, a new set of principal axes appear, and reorientation of the satellite occurs.

Deflection of a typical long, slender boom exposed to solar heating is depicted in Fig. 4. Here, the undeflected boom is assumed to lie along the U axis while the sun is assumed to be in the direction specified by the sun vector, σ. In the inertial frame the sun vector is defined by the expression

$$\sigma = \sin \alpha a_1 + \cos \alpha a_2 \tag{10}$$

where α is the sun angle or more explicitly the angle between the sun's vector and the normal to the satellite's orbital plane. The sun vector is also tilted so that the angle ξ between the sun's vector and the axis of the undeflected boom is given by the scalar product

$$\cos \xi = U \cdot \sigma \tag{11}$$

Thermal bending of the boom induced by solar heating is presumed to cause a tip deflection

$$Y_T = y_T \Gamma \tag{12}$$

whose direction Γ, is not only away from the sun and perpendicular to the U axis but is also in a plane that contains the sun's vector. The direction vector, Γ, is obtained from the vector triple product relationship

$$\Gamma = \frac{(\sigma \times U) \times U}{|(\sigma \times U) \times U|} \tag{13}$$

The tip deflection, y_T, for each boom is assumed to be the deflection that would be attained if all thermal lags were ignored. For a seamless, thin-walled cantilevered boom of circular cross-section the tip deflection can be approximated by the equation

$$y_T = \tfrac{1}{2} A_T \ell^2 \sin \xi [1 + \tfrac{1}{3} A_T \ell \cos \xi] \tag{14}$$

where ℓ = boom length, ft, and A_T is the thermal constant

$$A_T = (\alpha_0 e D J_s / 4hk) \tag{15}$$

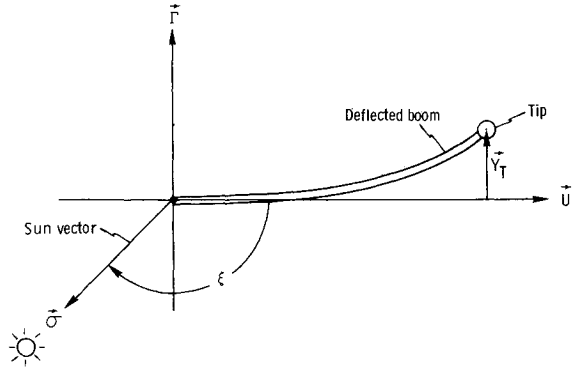

Fig. 4 Boom deflection.

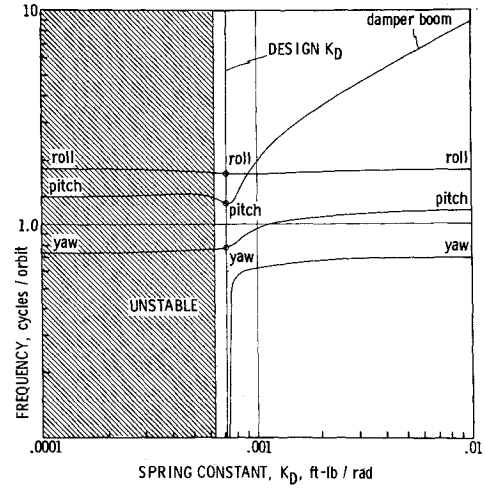

Fig. 5 Rigid body frequencies and linear stability boundary.

whose elements α_0 = absorptivity, D = boom diam, in.; e = linear thermal coefficient of expansion, in./in.-°F; h = thickness, in.; J_s = solar radiation intensity, BTU/hr-ft^2; k = thermal conductivity, Btu/hr-ft°F.

The tip deflection vectors for the main boom, side boom and damper boom are determined from the relationships of Eqs. (10-15). It should be noted that if the satellite is in the earth's shadow, solar radiation is ignored and y_T is set equal to zero. The sun model used for finding out whether the satellite is either in full sunlight or in the earth's shadow is described in Ref. 13.

Computed changes in the magnitudes and directions of the three tip deflections are used to rederive the dyadics $\tilde{\Phi}_{00}$, $\tilde{\Phi}_{10}$, $\tilde{\Phi}_{01}$, and $\tilde{\Phi}_{11}$ and subsequently to alter the torque elements on the right-hand side and the coefficient elements on the left-hand side of Eq. (8).

Results

The equations describing the quasi-static response of NRL 164 to solar radiation are basically represented by Eqs. (5, 8, 9 and 14). The representative first-order nonlinear differential equations of motion along with their associated supplementary equations have been programed for analysis on a digital computer. The solution is obtained through the use of Hamming's predictor-corrector method, with starting values determined by a Runge-Kutta procedure.

The essential aspects of the results presented here cover a selective investigation of the effect of boom thermal bending on the stability of the quasi-static model of NRL 164 in a circular orbit ($\epsilon = 0$). Particular emphasis has been placed on the influence of absorptivity, sun angle, and hinge stiffness on the satellite's responses in yaw, pitch, and roll.

Stability Criteria

Linearization of the satellite's nonlinear differential equations of motion provided a means of ascertaining the stability of NRL 164 in the absence of solar radiation. Stability, in this case, was determined by the character of the roots of the linearized equations. The resulting roots were either real or occurred in complex pairs with each imaginary pair corresponding to one of the satellite's rigid body frequencies. Linear stability criteria required that all of these roots have negative real parts.

The computed frequencies (obtained from the imaginary part of each root) are plotted in Fig. 5 for a variation in damper spring constant, K_D. All other satellite properties are consistent with Table 1. Despite strong coupling between rigid body motions in yaw, pitch, roll, and damper boom rotation, each frequency (as indicated in Fig. 5) can still be characterized by one of these rigid body motions.

As the spring becomes weaker a critical value is reached ($K_D = 0.00064$ ft-lb/rad) below which the real part of one of the roots becomes positive and an instability is revealed. In this region the destabilizing gravity gradient torque on the damper boom is large enough to overcome the damper spring torque and the satellite diverges from its initial orientation to a new, undesirable equilibrium position. For reference purposes, this divergence boundary delineates the region within which satisfactory operation of NRL 164 cannot be attained.

The stability of NRL 164 exposed to solar radiation was deduced through a time domain solution of the satellite's nonlinear differential equations of motion. In seeking a solution it was evident that nonlinearities in the simulation and economic limitations on computer usage would require a relatively imprecise definition of stability. The nonlinear stability criteria that was adopted assumed that the satellite was unstable if, after the model was initially perturbed by a set of "prime amplitude conditions" in yaw, pitch, and roll, a yaw inversion occurred within the first four orbits of the earth. The initial prime conditions selected were yaw = 30°; pitch = —30°; roll = —10°; and yaw, pitch, and roll rate = 0.

Basic Characteristics

The motions of NRL 164 in the absence of sunlight and initially perturbed by the prime conditions are plotted in Fig. 6. This figure serves as an instructive indicator of the basic nonlinear dynamic behavior of the nominal configuration and should be used in gaging the changes in response that are brought about by a parameter variation. As expected in this case, the satellite is very stable. Although yaw motions are initially quite large, they damp out rapidly and the system is close to an equilibrium attitude soon after the fourth orbit.

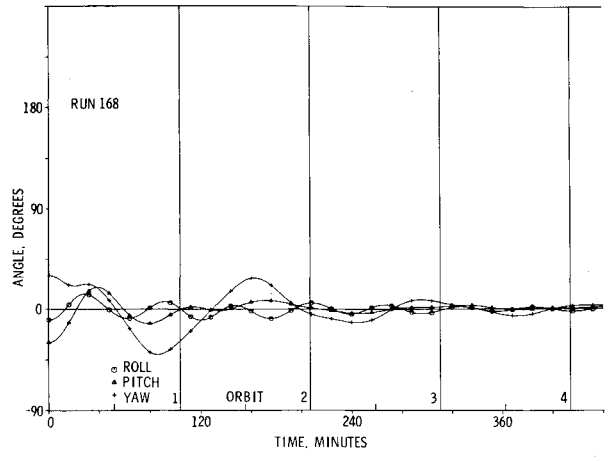

Fig. 6 Nominal satellite response, no sun.

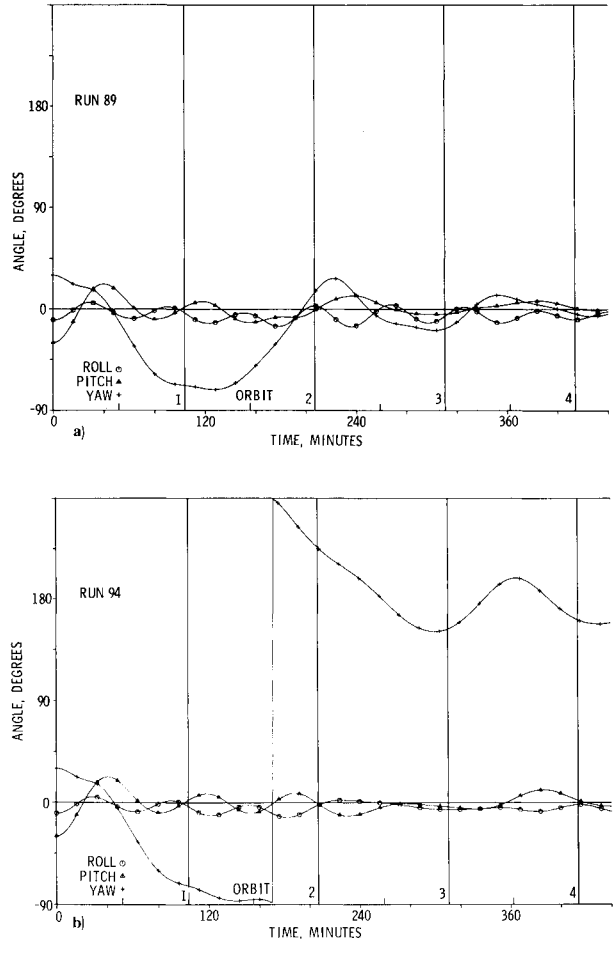

Fig. 7 Effect of absorptivity on response, $K_D = 0.000714$ ft-lb/rad, sun angle = 0°: a) absorptivity = 0.40; b) absorptivity = 0.45.

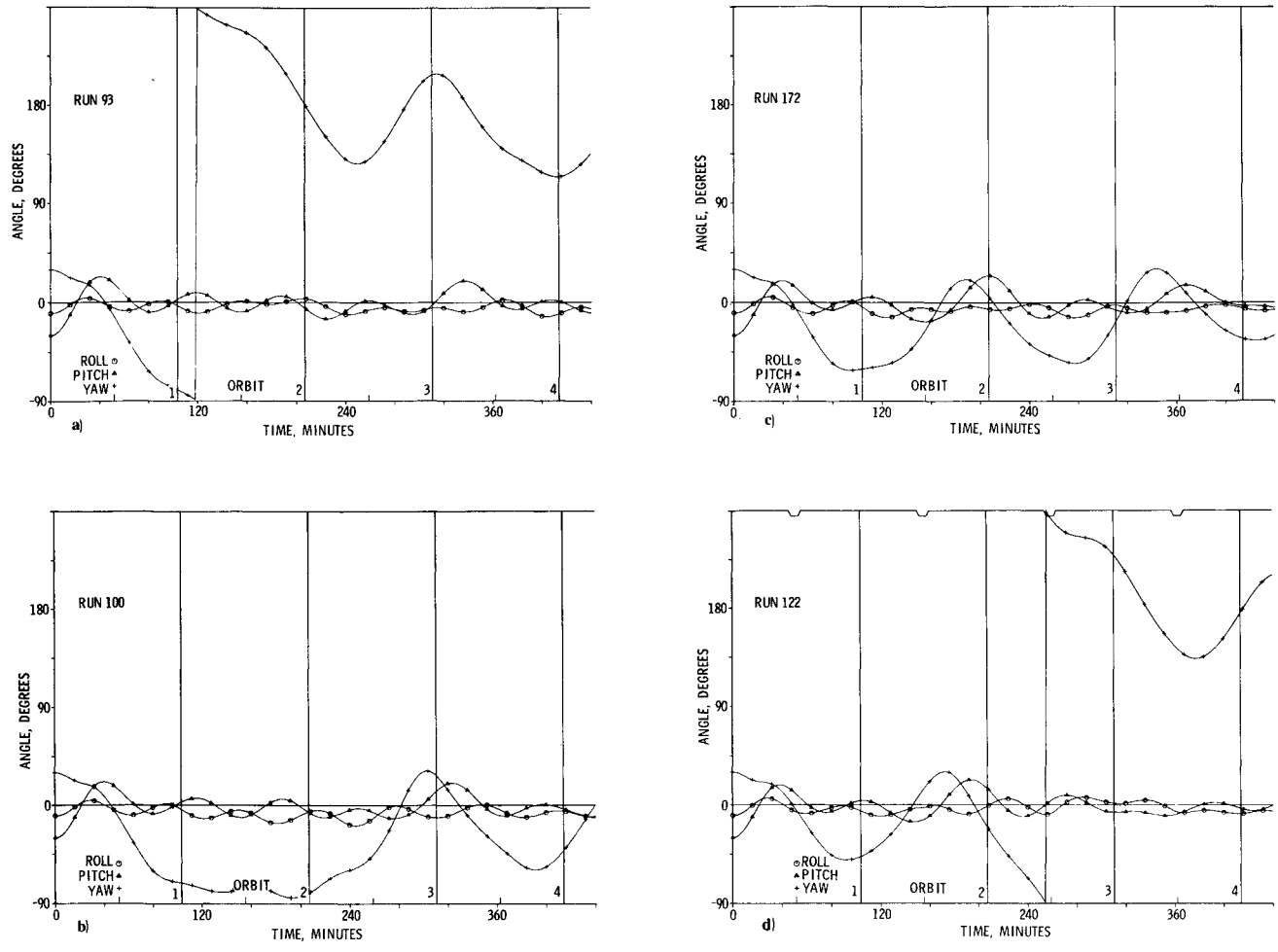

Fig. 8 Effect of sun angle on response, $K_D = 0.000714$ ft-lb/rad, absorptivity = 0.5: a) sun angle = 0°; b) sun angle = 10°; c) sun angle = 20°; d) sun angle = 30°.

Effect of Absorptivity

The present thermal instability supposition rests on the assumption that thermally induced changes in the satellite's inertial properties due to boom bending may cause a yaw instability. To examine this possitility, satellite responses were computed for variations in tip deflections [Eq. (14)], brought about by a change in absorptivity.

Since the outer surfaces of the booms were assumed to be highly reflective, a low absorptivity, $\alpha_0 = 0.13$, was specified as the nominal value. However, data accumulated by NASA's Goddard Space Flight Center [14] suggest that factors other than absorptivity tend to influence thermal bending, and large deflections may occur in spite of a low value of absorptivity. To compensate for these factors, an effective absorptivity of 0.5 was considered to represent the high end of the deflection scale.

The computed influence of absorptivity on the attitude motion of NRL 164 is illustrated in Fig. 7. For these responses in which the sun is normal to the orbital plane (sun angle at 0°) the plots reveal that the amplitude of yaw motion is particularly sensitive to a slight change in thermal distortion. For $\alpha_0 = 0.4$, the calculated yaw attitude, though large, seems to be stable. Conversely for $\alpha_0 = 0.45$, a yaw inversion occurs prior to the second orbit, and the configuration is considered to be unstable. The onset of an inversion appears to be closely dependent upon yaw reaching an angle of $-90°$.

Effect of Sun Angle

The observation of absorptivity led directly to the observation that the satellite's computed response and stability could be strongly influenced by a small change in sun angle. This was previously noted in the flight data [7] and now tends to be confirmed by the present quasi-static analysis.

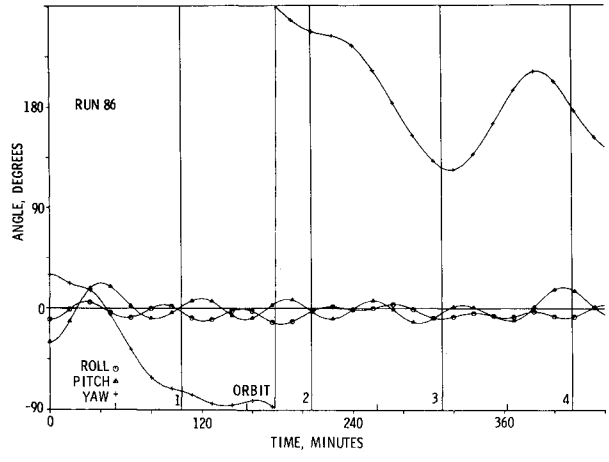

Fig. 9 Effect of hinge stiffness on response, $K_D = 0.0008$ ft-lb/rad, sun angle = 0°.

The sensitivity to a change in sun angle is typified by the computer plots shown in Fig. 8 which depict the yaw, pitch, and roll motions of NRL 164 for sun angles of 0°, 10°, 20°, and 30°. Here the magnitude of boom thermal absorptivity is 0.5, a value which for the 60 ft main boom and normal sun incidence results in a computed static tip deflection of approximately 5 ft.

In Fig. 8a, with the sun angle at 0°, a yaw inversion starts almost immediately and, as previously seen in Fig. 7 the satellite response is excessive. In Fig. 8b, however, just by shifting the sun angle to 10° the inversion is suppressed and the motion is surprisingly stable. In fact, in Fig. 8c, a further increase in the sun angle to 20°still leads to a stable configuration. Finally, in Fig. 8d, at a sun angle of 30° and after occultations† have begun, the computed response again indicates a yaw inversion. This inversion is probably involved with the deflection transient that arises as the satellite enters into the earth's shadow.

Effect of Hinge Stiffness

The comparison of most of the computed results with flight data is in itself quite good. As in flight, the controlling factor in establishing NRL 164's stability boundary appears to be most closely allied with sun angle. Hinge stiffness, however, also plays an important role in the results.

Some indication of the sensitivity of the computed response to a change in hinge stiffness is shown in Fig. 9 for a sun angle of 0° and $\alpha_0 = 0.4$. With a nominal hinge stiffness ($K_D =$ 0.000714 ft-lb/rad) the satellite's response is stable (see Fig. 7a). In Fig. 9, however, by increasing the hinge stiffness only about 10%, so that $K_D = 0.0008$ ft-lb/rad, the yaw response becomes too large.

Figures 10-12 illustrate how the computed quasi-static stability boundaries for sun angles of 0°, 10°, and 30° were influenced by variations in hinge stiffness (damper spring constant) K_D and absorptivity α_0. The illustrations essentially summarize the outputs from a large number of computer runs.

In these figures, the divergence region arises solely from the consideration that, in the absence of sunlight, the system becomes unstable for $K_D < 0.00064$ ft-lb/rad. Conversely the unstable regions that are shown in the figures encompass areas of yaw instabilities that were deduced by applying our nonlinear stability criteria.

In Figs. 10 and 11, the stability boundary is not only favorably influenced by a low value of hinge stiffness, but the stable region increases in area as the sun angle changes from 0° to 10°. For a sun angle of 30°, Fig. 12, the satellite passes through the earth's shadow, and the stability picture becomes quite confusing. Now the unstable regions are isolated into two pockets that restrict the onset of an instability to only certain limited combinations of absorptivity and hinge stiffness.

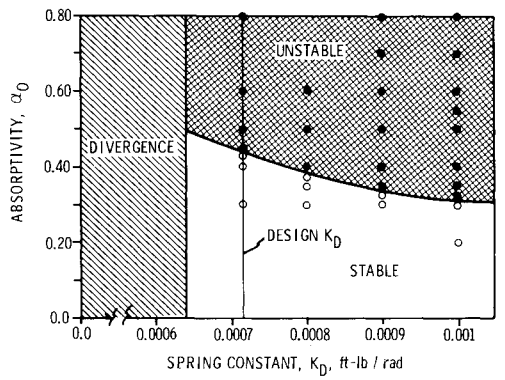

Fig. 10 Stability boundary for sun angle = 0°.

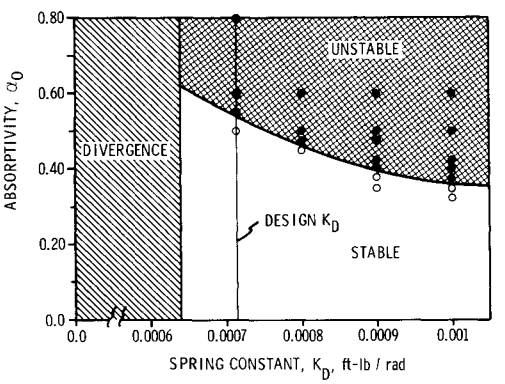

Fig. 11 Stability boundary for sun angle = 10°.

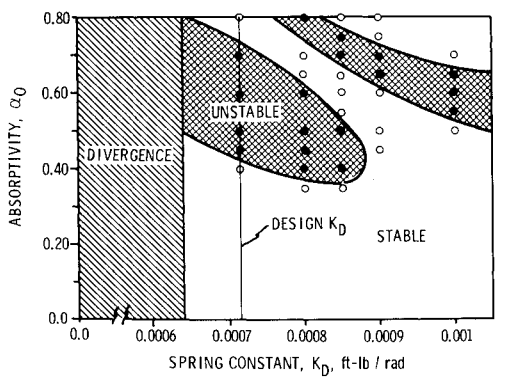

Fig. 12 Stability boundary for sun angle = 30°.

†Occultations are indicated by the downward facing steps in the horizontal line across the top of Fig. 8d.

Conclusions

Within the confines of relatively narrow stability criteria, it has been found that, under the quasi-static model, NRL 164 not only becomes unstable but, in a number of cases, responses were computed that closely resembled flight data.

From a review of the results, it has been discovered that: 1) The onset of a yaw instability is particularly sensitive to a small change in sun angle, with the least favorable sun angle at 0°. 2) In order to obtain an adverse effect from thermal distortion, it was necessary to assume a larger thermal deflection than might be inferred from a boom's nominal thermal properties. Some evidence is available, however, to justify this assumption.[14] 3) Occultation of the satellite produces isolated regions of instabilities believed to be related to the abrupt changes in boom deflections that occur as the satellite enters or leaves the earth's shadow. 4) In most cases, an increase in hinge stiffness tends to be destabilizing. This is probably due to a corresponding reduction in energy removal as the damper boom rotational frequency increases.

By comparing the data collected during the computer study, it has been concluded that the quasi-static approach provides a valid means of predicting the anomalous behavior of NRL 164. In retrospect, the analysis probably could have been used to anticipate the instability seen in the flight data of NRL 164.

If three-axis gravity gradient stabilization of a satellite through the use of long, slender booms is to be considered in future spacecraft designs, adequate consideration must be given to the influence of thermal distortion on system performance. Assuming that such satellites are still of practical consequence, it is important that the designer have available a means of selecting configurations that are free from the thermally induced instabilities.

References

[1] DeBra, D.B., "The Large Attitude Motions and Stability, Due to Gravity, of a Satellite with Passive Damping in an Orbit of Arbitrary Eccentricity about an Oblate Body," SUDAER No. 162, 1962, Ph. D. dissertation, Dept. of Aeronautics and Astronautics, Stanford University, Stanford, Calif.

[2]Fletcher, H.J., Rongved, L., and Yu, E.Y., "Dynamics Analysis of a Two-Body Gravitationally Oriented Satellite," *Bell System Technical Journal,* Sept. 1963, pp. 2239-2266.

[3]Raymond, F.W., "Gravity Gradient Torques on Artificial Satellites," *Astronautica Acta,* Vol. 12, No. 1 1966, pp. 33-38.

[4]Hartbaum, H., Hooker, W., Leliakov, I., and Margulies, G., "Configuration Selection for Passive Gravity Gradient Satellites," *Symposium on Passive Gravity Gradient Stabilization,* SP-107, May 1965, NASA.

[5]Barba, P.M. and Marx, S.G., "An Integrated 3-Axis Gravity Gradient Stabilization System," *Symposium on Gravity Gradient Attitude Control,* Aerospace Corp., El Segundo, Calif., Dec. 1968.

[6]"Design and Performance of an Integrated, Hysteresis Damped, Gravity Stabilized Satellite," TR-DA 2091, July 1969, Space and Re-Entry Systems Div., Philco-Ford Corp., Palo Alto, Calif.

[7]Goldman, R.L., "Examination of the Anomalous Behavior of Three Gravity Gradient Satellites," TR-71-07c, March 1971, Martin Marietta Corp., Baltimore, Md.

[8]Frisch, H.P., "Coupled Thermally-Induced Transverse Plus Torsional Vibrations of a Thin-Walled Cylinder of Open Section", TR R-333, March 1970, NASA.

[9]Hooker, W.W., "A Set of r Dynamical Attitude Equations for an Arbitrary n-Body Satellite having r Rotational Degrees of Freedom," *AIAA Journal,* Vol. 8, July 1970, pp. 1204-1207.

[10]Kanning, G., "The Influence of Thermal Distortion on the Performance of Gravity Stabilized Satellites," TN D-5435, Nov. 1969, NASA.

[11]Tinling, B.E. and Merrick, V.K., "Exploitation of Inertial Coupling in Passive Gravity Gradient Stabilized Satellites," *Journal of Spacecraft and Rockets,* Vol. 1, July-Aug. 1964, pp. 381-387.

[12]Constant, F.W., *Theoretical Physics,* Addison-Wesley, Reading, Mass., 1954.

[13]Goldman, R.L., "Instability of a Gravity Gradient Satellite Due to Thermal Distortion," CR-2516, March 1975, NASA.

[14]Herzl, G.G., Walker, W.W., and Ferrera, J.D., "Tubular Spacecraft Booms (Extendable, Reel Stored)," SP-8065, Feb. 1971, NASA.